JPE 19-2-14

https://doi.org/10.6113/JPE.2019.19.2.487
ISSN(Print): 1598-2092 / ISSN(Online): 2093-4718

Voltage Balance Control of Cascaded H-Bridge Rectifier-Based Solid-State Transformer with Vector Refactoring Technology in αβ Frame

Hui Wong†, Wendong Huang*, and Li Yin*

†,*School of Electrical Engineering, Guangxi University, Nanning, China

Abstract

For a solid-state transformer (SST), some factors, such as signal delay, switching loss and differences in the system parameters, lead to unbalanced DC-link voltages among the cascaded H-bridges (CHB). With a control method implemented in the αβ frame, the DC-link voltages are balanced, and the reactive power is equally distributed among all of the H-bridges. Based on the αβ frame control, the system can achieve independent active current and reactive current control. In addition, the control method of the high-voltage stage is easy to implement without decoupling or a phase-locked loop. Furthermore, the method can eliminate additional current delays during transients and get the dynamic response rapidly without an imaginary current component. In order to carry out the controller design, the vector refactoring relations that are used to balance DC-link voltages are derived. Different strategies are discussed and simulated under the unbalanced load condition. Finally, a three-cell CHB rectifier is constructed to conduct further research, and the steady and transient experimental results verify the effectiveness and correctness of the proposed method.

Key words: $\alpha\ \beta$ frame control, Cascaded H-bridge rectifier, Solid-state transformer, Voltage and power balance, Vector refactoring

I. INTRODUCTION

In the past few decades, motivated in part by the success of smart grids and the energy Internet, the solid-state transformer (SST) has attracted a lot of attention [1]. The SST can also be called a power electronic transformer (PET) or a universal transformer [2], [3]. It offers better performance in terms of size and weight, and has the features of electrical isolation, harmonic isolation, voltage conversion, renewable energy access, and power factor correction [4], [5]. Future electric power distribution systems should be designed to promote the plug-and-play interface of distributed renewable energy and distributed energy storage devices. This new type of transformer is expected to be widely applied to the energy Internet [6], [7].

Researches at North Carolina State University presented the configuration of a three-stage 20-kVA SST in [8], which consists of a rectifier stage, an isolated stage and an inverter stage. Feng et al. [9] presented a review of the SST based on railway traction systems with unique application features and requirements. Zhao et al. [10] focus on the isolated stage of the SST. Generally speaking, the three-stage SST has attracted a lot of attention in multiple topologies [11].

The normal operation of the rectifier stage is the key to a three-stage SST. Multilevel converters applied to the rectifier stage are becoming increasingly popular because due in large part to their unique advantages over two-level converters, such as lower switching stress during the turn on and turn off of semiconductor devices, less reverse voltage, lower current rating, lower rating filter requirement, etc. [12], [13]. The CHB rectifier achieves a better performance over other multilevel converters due to its advantages in terms of modular structure, fewer switching devices, and independent unit of the DC side [14], [15].

In view of the CHB rectifier, one of the main issues is to achieve voltage balance. Given the differences in the power losses and pulse delay, there is a divergence in the power conversion among cells [3], [16], [17]. For the DC-link voltage of each CHB, it is desirable to be the same as the voltage reference.

Common DC-link voltage balance methods of the CHB

Manuscript received Apr. 25, 2018; accepted Jan. 11, 2019
Recommended for publication by Associate Editor Honnyong Cha.
†Corresponding Author: wanghui_5524@163.com
Tel: +86-771-3233178, Guangxi University
*School of Electrical Engineering, Guangxi University, China

rectifier stage can be divided into two types. 1) Utilizing the redundant switching vectors in the modulation [18]-[20]. 2) Adding a voltage balance controller to the original system [21]-[27]. The first type requires a central switching controller. However, it is difficult for a system to extend higher voltage levels with an increasing amount of redundant states. The second type typically regulates the active power controlled by each of the H-bridges to individually balance the DC-link voltage. This paper uses the second type of voltage balance method with αβ frame control.

In this paper, a control method in the αβ frame is presented to achieve the following objectives.

1) Balancing the DC-link voltage and forming a reasonable power distribution for each of the H-bridges in the rectifier stage of SSTs.
2) Reactive power compensation for SSTs.
3) Simplifying the control structure, lessening the calculative burden and achieving a better transient-state performance.

Conventionally, the second type of method mainly focuses on the unbalance issues in the d-q coordinate system. Single phase d-q coordinate control is applied in the rectifier, which needs to implement a stationary-to-rotating coordinate transform (αβ to d-q) with the aid of an imaginary current. Usually, a phase-locked loop (PLL) and coordinate transform are used in the d-q coordinate system, which increases the calculation burden of embedded processor [27], [28].

In addition, a d-q double closed-loop system needs decoupling control. It is easy to bring coupling effects to a system due to the additional voltage balance controller. For some reported control methods, an *N*-cell CHB rectifier has *N* voltage regulators. A generalized per-phase DC-link voltage balance control strategy of a three-phase STATCOM is presented in [21]. In [22], the unbalanced-load correction of a three-phase three-stage PET with nine voltage regulators is presented. However, no attempt is made to identify or eliminate the coupling effect between the voltage balance controller and the original closed-loop system [21], [22].

When compared with [21], some improvements have been made in relevant studies. For instance, an *N*-cell CHB rectifier is controlled by (*N*-1) individual DC-link voltage regulators. Furthermore, a reduction in the coupling effect between the voltage balance controller and the d-q control system is implemented in [23]. The conditions that eliminate the coupling effect between the voltage balance control and double closed-loop system are identified in [24]. However, the dynamic performance of the input current is not good when a proportional integral (PI) controller is used. A proportional-resonant (PR) controller is applied to track the AC reference signal with zero steady-state error in this paper.

The rectifier stage of an SST also has reactive power compensation capability. In [25], the sign of the active power reference is used in the voltage balance controller for a CHB. Therefore, it is obviously an insufficiency that reactive power control is often neglected.

In this paper, a method for the voltage balance and power control for the *N*-cell CHB rectifier stage of an SST in the αβ frame is used. The main technical route is adding the compensation components of the duty cycle vectors to the common duty cycle to reconstruct the duty cycle vectors. (*N*-1) DC voltage regulators are coordinated with each other according to the vector relations. Therefore, *N* compensation components are generated without decoupling. In particular, the duty cycle regulates the DC-link voltage balance while the relationship of the power distribution is also considered. The voltage balance controller maintains a uniform distribution of the reactive power, and it distributes the active power according to the demands of *N*-cell H-bridges. In experiments, when compared with the d-q coordinate control, the αβ frame control shows better dynamic performance and eliminates the additional current delay in transients. The phase difference between the grid voltage and current changes with the alteration of the current reference. It is confirmed that rectifier stage of the SST is capable of realizing independent control of the active and reactive power. Generally speaking, the αβ frame control only needs an imaginary voltage component. It does not require an imaginary current component or a PLL, which simplifies the control structure.

This paper is organized as follows. First, the modeling of the SST is introduced in section II. Next, a new principle of voltage and power control is presented in section III. Section IV shows simulations and experimental results that verify the proper operation of the CHB rectifier. Finally, section V concludes this paper.

II. Model of a Three-Stage SST

A. Rectifier Stage of an SST Based on the CHB Topology

Fig. 1 shows the configuration of a three-stage SST. The SST consists of a CHB rectifier, dual active bridge (DAB) converters with high-frequency transformers and an output stage with a parallel-connected H-Bridge. Where u_s is the input voltage, i_s is the input current, u_{dci} is the i_{th} H-bridge DC-link voltage, i_{oi} is the input current of the DAB converter, L is the input inductance, and C_i is the DC capacitance. The symbol i is the serial number of each H-bridge (i=1, 2, 3).

Where, u_{ab} is defined as the PWM voltage of the CHB rectifier. Therefore, seven distinct AC voltage levels u_{an} can be applied to the AC input terminal between points "*a*" and "*b*". Since all of the H-bridges are connected in series, the instantaneous total PWM voltage of the CHB rectifier is equal to the sum of the individual H-bridge AC voltages.

$$u_{ab} = u_1 + u_2 + u_3 \tag{1}$$

Mathematical analyses of a three-cell CHB rectifier have been carried out. The differential equations of the CHB rectifier are described as follows:

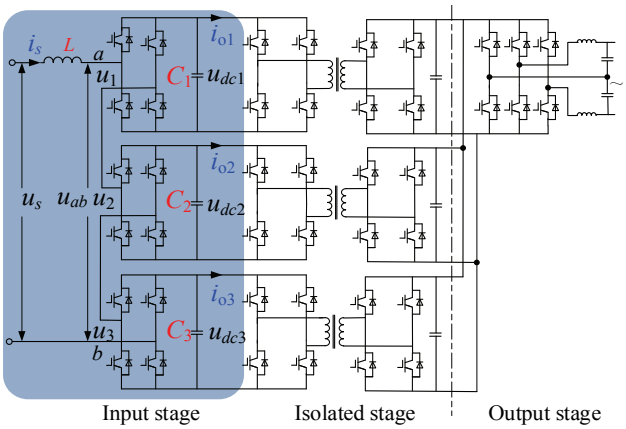

Fig. 1. Configuration of a CHB based SST.

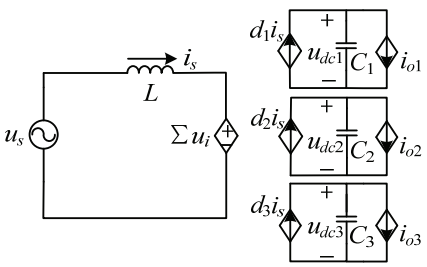

Fig. 2. Switching model of a CHB.

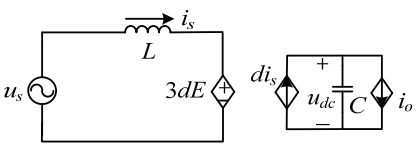

Fig. 3. Average model of a CHB.

$$L\frac{di_s}{dt} = u_s - u_{ab} \tag{2}$$

$$d_i i_s = C_i \frac{du_{dci}}{dt} + i_{oi} \tag{3}$$

$$S_i = \begin{cases} 0; & \begin{cases} 0 \le \omega_s t \le (1-d_i)\pi \\ (1+d_i)\pi \le \omega_s t \le 2\pi \end{cases} \\ 1; & (1-d_i)\pi \le \omega_s t \le (1+d_i)\pi \end{cases} \tag{4}$$

Where, S_i is the switching function of the H-bridge, d_i is the duty cycle of the H-bridge, $\omega_s=2\pi f_s$, f_s is the switching frequency, and t is the sampling time. The switching model can be shown in Fig. 2. Then the Fourier transform for S_i can be expressed as follows:

$$S_i = d_i + \sum_{n=1}^{\infty} (-1)^n \frac{2}{n\pi} \sin(nd_i\pi)\cos(n\omega_s t) \tag{5}$$

Then the H-bridge AC voltage can be expressed as:

$$u_i = u_{dci} d_i \tag{6}$$

The average model is given in Fig. 3. For the sake of simplicity, it is assumed that the power loss differences among the different converter modules are the same and very small. They are neglected in the average model. Ideally, it is concluded that u_{dc1}, u_{dc2} and u_{dc3} are equal to E when the parameters of the H-bridge are the same. E is the DC-link reference voltage of each H-bridge. The value of d_i for each of the H-Bridges is replaced by a common duty cycle d.

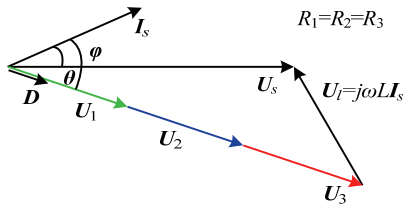

Fig. 4. Voltage vectors under balanced load condition.

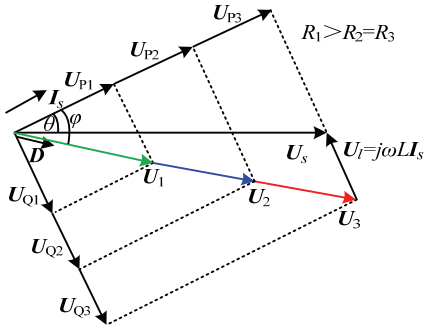

Fig. 5. Voltage vectors under unbalanced load condition.

B. Imbalanced Analysis of a CHB Rectifier

Unbalanced DC-link voltages cause capacitance or IGBT device over-voltage and trigger system overvoltage protection. The unbalanced power causes device over-current and results in unbalanced heat distributions. The conventional control in a double closed-loop system is mainly based on d-q coordinates, and maintains the DC-link voltage balance among all of the H-bridges by a common duty cycle d. In reality, the DC-link voltages become unequal when the loads are different. Once the DC-link voltages increase, the power switch fails or the input current becomes highly distorted.

The CHB rectifier PWM voltage vector is the sum of all the H-bridge AC voltage vectors. As shown in Fig. 4, the constraints of the voltage vectors are given by (1) and (6) when the loads are the same. Where, U_i is the i_{th} H-bridge AC voltage vector, I_s is the single-phase input current vector, and U_s is the single-phase input voltage vector. D generated by a double-loop is defined as the common duty cycle vector. Fig. 5 shows voltage vectors under unbalanced load condition. U_{Pi} is the projection of voltage in the active direction, U_{Qi} is the projection of voltage in the reactive direction, θ is the angle between the grid voltage and current, and φ is the angle between the current and common duty cycle. The complex power provided by the power grid can be expressed as:

$$S_s = P_s + jQ_s = U_s I_s \cos\theta + jU_s I_s \sin\theta \tag{7}$$

The power unbalance among the different H-bridges can be simply induced by the unequal resistance R_i paralleled with the DC-link capacitance. According to the linear modulation theory, the active power P_i and reactive power Q_i on the DC side of the CHB are calculated as:

$$S_i = P_i + \mathrm{j}Q_i = \frac{{u_{dci}}^2}{R_i} + \mathrm{j}C_i u_{dci}\frac{du_{dci}}{dt} \tag{8}$$

Assuming that the losses are negligible, the input power on the AC side is equal to the output power on the DC side. Hence:

$$\begin{cases} P_i = U_i I_s \cos\varphi_i = u_{dci} D_i I_s \cos\varphi_i \\ Q_i = U_i I_s \sin\varphi_i = u_{dci} D_i I_s \sin\varphi_i \end{cases} \tag{9}$$

The derivations are based on the assumption of one double closed-loop system. Where, φ_i is the angle between the current and U_i. In addition, D_i of each H-bridge is equal to D. Substitute D into (9) and (10). Then the DC-link voltage u_{dci} meets the following relation:

$$\frac{u_{dci}}{R_i} = DI_s \cos\varphi \tag{10}$$

Thus, the relation between the DC-link voltage u_{dci} and R_i is as follows:

$$\frac{u_{dc1}}{R_1} = \frac{u_{dc2}}{R_2} = \cdots = \frac{u_{dcN}}{R_N} \tag{11}$$

Substitute the derived result from (11) into (9). In the case of one double closed-loop system, the greater the resistance becomes, the greater the DC-link voltage u_{dci}, the active power and the reactive power become (as shown in Fig. 5). In other words, although the total voltage is still controlled by the double closed-loop system, the unbalanced voltage distribution among the cascaded H-bridges exists. Specifically, in order to balance the DC-link voltages among the cascaded H-bridges, a modification of the duty cycle is added to the d to form d_i for each of the H-bridges.

Reactive power is calculated as:

$$Q_i = C_i u_{dci}\frac{du_{dci}}{dt} \tag{12}$$

Reactive power is influenced by DC ripple voltage when u_{dci} is regulated to the reference voltage. According to [23], a voltage balance controller is added to the double closed-loop system in d-q coordinates. The analysis shows that the introduction of a voltage balance controller produces a coupling effect on the double closed-loop d-q coordinate system. Differential equations of a CHB rectifier with basic double closed-loop control in the d-q coordinates can be described as follows:

$$\begin{cases} L\dfrac{di_{sd}}{dt} = \omega L i_{sq} + u_{sd} - d_d N u_{dca} \\ L\dfrac{di_{sq}}{dt} = \omega L i_{sd} + u_{sq} - d_q N u_{dca} \end{cases} \tag{13}$$

Where, u_{dca} is the average value for all of the DC-link voltages, u_{sd} and u_{sq} are the d-axis and q-axis components of the input voltage u_s, d_d and d_q are the d-axis and q-axis duty cycles, and i_{sd} and i_{sq} are the d-axis and q-axis input inductance currents, respectively. When the DC-link voltages are unbalanced, the differential equations of the double closed-loop system are transformed into the following:

$$\begin{cases} L\dfrac{di_{sd}}{dt} = \omega L i_{sq} + u_{sd} - d_d N u_{dca} + (d_d N u_{dca} - \sum_{i=1}^{N} d_{di} u_{dci}) \\ L\dfrac{di_{sq}}{dt} = \omega L i_{sd} + u_{sq} - d_q N u_{dca} + (d_q N u_{dca} - \sum_{i=1}^{N} d_{qi} u_{dci}) \end{cases} \tag{14}$$

Comparing (13) with (14), $d_d N u_{dca} - \sum_{i=1}^{N} d_{di} u_{dci}$ and $d_q N u_{dca} - \sum_{i=1}^{N} d_{qi} u_{dci}$ are additional terms generated by the voltage balance controller.

C. αβ Frame Control

In general, adding a voltage balance controller to a d-q double closed-loop system makes it necessary to solve the coupling effect between the voltage balance controller and the original system. In addition, using a voltage balance controller to maintain a balanced DC-link voltage in d-q coordinates needs a PLL and a coordinate transform. Thus, this paper presents a new type of control method in the αβ frame without decoupled d-q vector control or an imaginary current. The amplitude of $u = (u_\alpha, u_\beta)^{\mathrm{T}}$ is a constant that can be described as:

$$|u| = \sqrt{{u_\alpha}^2 + {u_\beta}^2} \tag{15}$$

Where, u_α and u_β represent the components of u in the αβ frame; projections of u_s in an αβ frame system are made to obtain the voltage unit vectors (v_α, v_β); u_α and u_s are in phase and have same amplitude; and an imaginary voltage u_β that is lagging the grid u_s by 90° is generated by u_s through a second order generalized integrator (SOGI). The unit vectors are derived as:

$$\begin{bmatrix} v_\alpha \\ v_\beta \end{bmatrix} = \frac{1}{|u|}\begin{bmatrix} u_\alpha \\ u_\beta \end{bmatrix} \tag{16}$$

A control block in the αβ frame is shown in Fig. 6, and this block consists of a double closed-loop control, a unit voltage control and a voltage balance control. In this case, the active current reference i_{sp}^* is the output of the voltage loop PI regulator; the reactive current reference i_{sq}^* is directly given; the outer voltage loop regulates the total DC voltage; the errors between the measured current i_s and current reference i_s^* are input to the PR regulator that can track the AC reference signal with zero steady-state error; and d is generated by the PR regulator and is integrated with Δd_i (modulation generated by the voltage balance controller) to form d_i for each H-bridge.

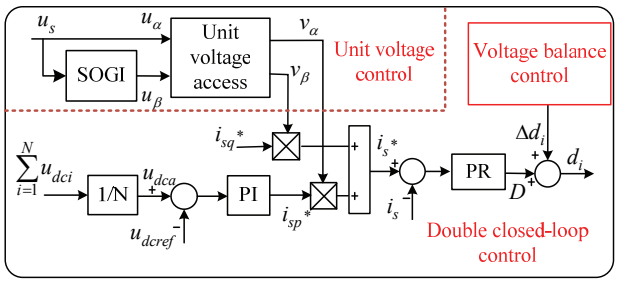

Fig. 6. Double closed-loop system in the αβ frame.

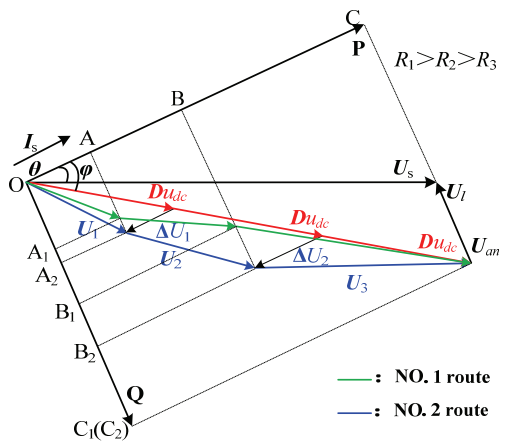

Fig. 7. Comparison of two different balance controls.

III. Method Based on Vector Refactoring

The balance control of a CHB rectifier is shown in Fig. 7. The refactoring duty cycle is to correct small changes in the modulated duty cycle during this process. The voltage loop control is to make the DC-link voltage of each independent H-bridge track the average voltage of all the H-bridges so as to balance the DC-link voltage. A comparison of two different approaches for voltage and power control is shown in Fig. 7. The red route indicates the common duty cycle modulation strategy in a double closed-loop system. The difference between NO.1 route and NO. 2 route is that NO. 2 route also considers the reactive power balance in addition to the voltage balance.

If the DC-link voltages among the H-bridges are balanced, the geometric relation in Fig. 7 can be derived from (10).

$$\mathrm{OA}:\mathrm{AB}:\mathrm{BC}=\mathrm{P}_1:\mathrm{P}_2:\mathrm{P}_3=\frac{1}{R_1}:\frac{1}{R_2}:\frac{1}{R_3} \tag{17}$$

The relation of the reactive power among the H-bridges in NO.1 route is:

$$\mathrm{OA}_1:\mathrm{A}_1\mathrm{B}_1:\mathrm{B}_1\mathrm{C}_1=\mathrm{Q}_1:\mathrm{Q}_2:\mathrm{Q}_3 \tag{18}$$

The active duty cycle is only adjusted to achieve the DC-link voltage balance, while the reactive power balance is not realized.

The relation of the reactive power among the H-bridges in NO.2 route is:

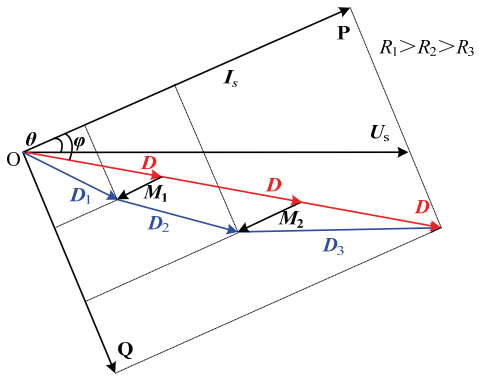

Fig. 8. Duty cycle vector under balance control.

$$\mathrm{OA}_2=\mathrm{A}_2\mathrm{B}_2=\mathrm{B}_2\mathrm{C}_2 \tag{19}$$

The common duty cycle exerts the same effect on each of the H-bridges. Therefore:

$$\mathrm{Q}_1=\mathrm{Q}_2=\mathrm{Q}_3 \tag{20}$$

From the vector analysis, one conclusion is derived. The reactive power balance can be achieved on the basis of the voltage balance.

ΔU_1 and ΔU_2 are compensation voltages. According to the vector relationship, the following equation is established:

$$\begin{cases} \boldsymbol{D}u_{dc}+\Delta\boldsymbol{U}_1=\boldsymbol{U}_1 \\ \boldsymbol{D}u_{dc}+\Delta\boldsymbol{U}_2-\Delta\boldsymbol{U}_1=\boldsymbol{U}_2 \\ \boldsymbol{D}u_{dc}-\Delta\boldsymbol{U}_2=\boldsymbol{U}_3 \end{cases} \tag{21}$$

Thus, the relation of the duty cycle vectors is shown in Fig. 8.

$$\begin{cases} \boldsymbol{D}+\boldsymbol{M}_1=\boldsymbol{D}_1 \\ \boldsymbol{D}+\boldsymbol{M}_2-\boldsymbol{M}_1=\boldsymbol{D}_2 \\ \boldsymbol{D}-\boldsymbol{M}_2=\boldsymbol{D}_3 \end{cases} \tag{22}$$

Where, M_1 and M_2 are generated by DC voltage regulators, and have a direction that is opposite that of the input current. This relation of the duty cycle vectors can also be applied to an N-cell CHB.

$$\begin{cases} \Delta\boldsymbol{D}_i=\boldsymbol{M}_i-\boldsymbol{M}_{i-1} \\ \boldsymbol{D}_i=\boldsymbol{D}+\Delta\boldsymbol{D}_i \\ \boldsymbol{U}_{ani}=u_{dci}\boldsymbol{D}_i \end{cases} \qquad 1\le i\le N \tag{23}$$

It should be noted that (23) provides the fundamental relations among the modification values of the duty cycles for an N-cell CHB rectifier. ΔD_i and D_i are the vectors of Δd_i and d_i, respectively. Δd_i is added to the original d, and d_i for the i_{th} H-bridge is adjusted. The active power is redistributed to eliminate voltage unbalance. Δd_1 for the first H-bridge is equal to M_1, Δd_N for the last H-bridge is equal to $(-M_{N\text{-}1})$, and $M_N=0$.

$$\begin{cases} \Delta d_i=M_i-M_{i\text{-}1} \\ \Delta d_N=-M_{N\text{-}1} \end{cases} \tag{24}$$

Only (N-1) DC voltage regulators are used to maintain the DC-link voltage balance for an N-cell CHB rectifier. The idea

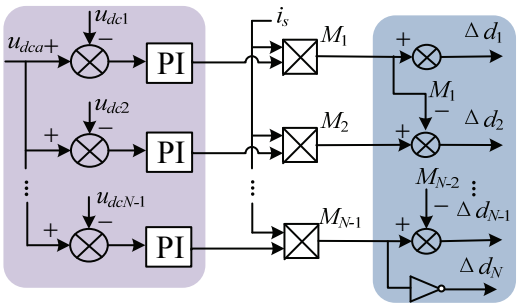

Fig. 9. Voltage balance control for a CHB.

TABLE I
SIMULATION PARAMETERS OF THE SYSTEM

Parameters	Value
Grid voltage (u_s)	220 V
Grid frequency (f)	50 Hz
Input inductance (L)	3.0 mH
DC-link total voltage (u_{dc})	400 V
DC-link capacitance(C)	4700 μF
DC-link load resistance (R_i)	15 Ω
Cell number of H-Bridge	3

is to adjust the duty cycle for each of the H-bridges so the distributions of the total transferred power are guaranteed. Hence:

$$\sum_{i=1}^{N}\Delta d_i = M_1 + (-M_1+M_2) + \cdots + (-M_{n-2}+M_{n-1}) - M_{n-1} = 0 \quad (25)$$

$$\begin{cases} \mathrm{P}_i = (Du_{dc} + \Delta U_i - \Delta U_{i-1}) I_s \cos\varphi_i \\ \mathrm{Q}_i = u_{dc} D I_s \sin\varphi \end{cases} \quad 1 \le i \le N \quad (26)$$

Therefore, the total DC-link voltage regulation is not affected. Meanwhile, the projection of ΔU_i in the reactive axis is zero, which means the active power is distributed as per demand and the reactive power is not affected. Fig. 9 shows the voltage balance control based on equation (23).

IV. SIMULATION AND EXPERIMENTAL RESULTS

A. Simulation Results

To verify the DC-link voltage balance and power control for a three-cell CHB rectifier under unbalanced load conditions, two different control strategies are simulated in the capacitive mode. In the simulation case, the DC-link voltage is regulated to the reference 400 V total (133 V per H-bridge) and the single-phase input voltage is 50 Hz 220 V.

The main parameters for the system are shown in Table I. Fig. 10 shows the DC-link voltages of the three-cell CHB without a voltage balance controller. Initially, all of the DC-link load resistances are same and equal to 15 Ω. Then at time t =1.0 s, the DC-link load resistance connected to the third H-Bridge is changed to 10 Ω. Before 1.0 s, the three H-bridges

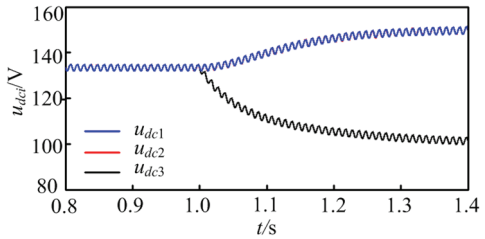

Fig. 10. DC-link voltages without a voltage balance controller.

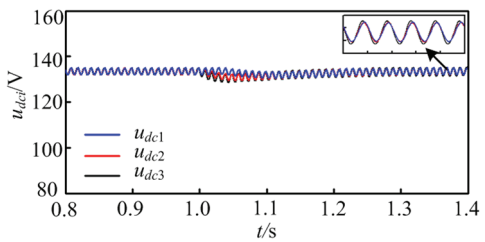

Fig. 11. DC-link voltages with a voltage balance controller.

transform the same amount of DC voltage, $u_{dc1} = u_{dc2} = u_{dc3}$ =133 V. However, after the third load resistance is changed, u_{dc1} and u_{dc2} are increased, but u_{dc3} is decreased. The summation of all the DC-link voltages is equal to the setting. The H-bridge connected with the smaller resistance has a lower DC-link voltage.

Fig. 11 shows three DC-link voltages with voltage balance control (the strategy shown in Fig. 9 is implemented), and the injection of a 10 A reactive current i_{sq}^*. Initially, the voltage balance control is activated. It can be seen that the three DC-link voltages are balanced. At 1.0 s, the DC-link load resistance connected to the third H-bridge is changed to 10 Ω. As shown in Fig. 11, the voltage balance control is achieved even with an unbalanced resistance. A partial zoomed view of the DC-link voltages is shown in Fig. 11. With the voltage balance control built in the αβ frame system in this paper, the controller is able to quickly bring voltages back to the setting. Obviously, the DC ripple voltages of the three-cell CHB rectifier are nearly same as those in Fig. 11. Therefore, the reactive power that is supplied by each of the H-bridges to the grid remains identical. This conclusion matches well with the one presented in [26], which verifies the potential for the equal distribution of reactive power.

B. Experiment Results

To verify the voltage balance and power control in the αβ frame, an experiment platform of a three-cell CHB rectifier has been implemented. The proposed algorithm is implemented by a TMS320F28377D (32-bit floating-point processor). The CHB rectifier is connected to the utility grid voltage through a coupling transformer and a voltage regulator, which ensures the safety of the experimental equipment. The DC-link voltage reference is regulated to the reference 150 V in total (50 V per H-bridge).

In order to compare d-q coordinate control with αβ frame

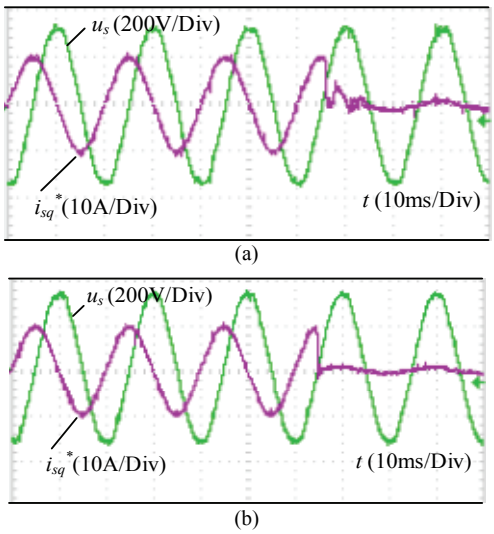

Fig. 12. Step current reference change of the capacitive mode. (a) d-q coordinate control. (b) αβ frame control.

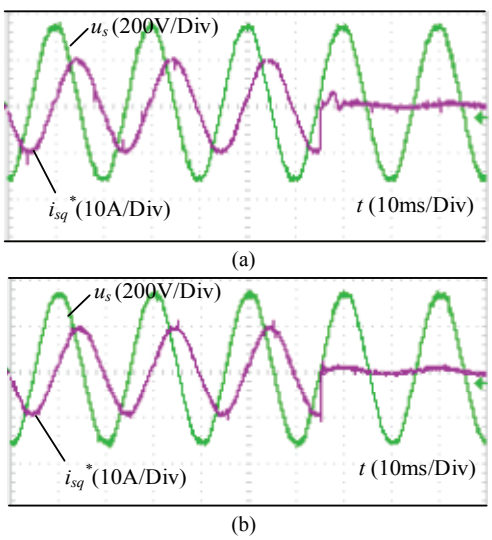

Fig. 13. Step current reference change of the inductive mode. (a) d-q coordinate control. (b) αβ frame control.

control in terms of transient-state response, a step reactive current reference (change i_{sq}^*) is changed in both coordinate controls. To compare in an easier way, a step-change signal is triggered by the zero-crossing detection of post-processing blocks in the TMS320F28377D. The capacitance and resistance that are connected to the DC bus of each H-bridge are substituted to the DC source at this moment. i_{sq}^* is stepped from 10A and -10A to 0. In terms of Fig. 12 and Fig. 13, the αβ frame control makes the system respond rapidly, and can exactly track the new current reference within 1ms.

Fig. 14 shows experimental results of the three-cell CHB rectifier under balanced load conditions. The CHB rectifier stage of the SST converts the input AC voltage into the regulated DC voltages and has reactive power compensation capability. The reactive current reference can be generated and communicated to the TMS320F28377D controller. After the

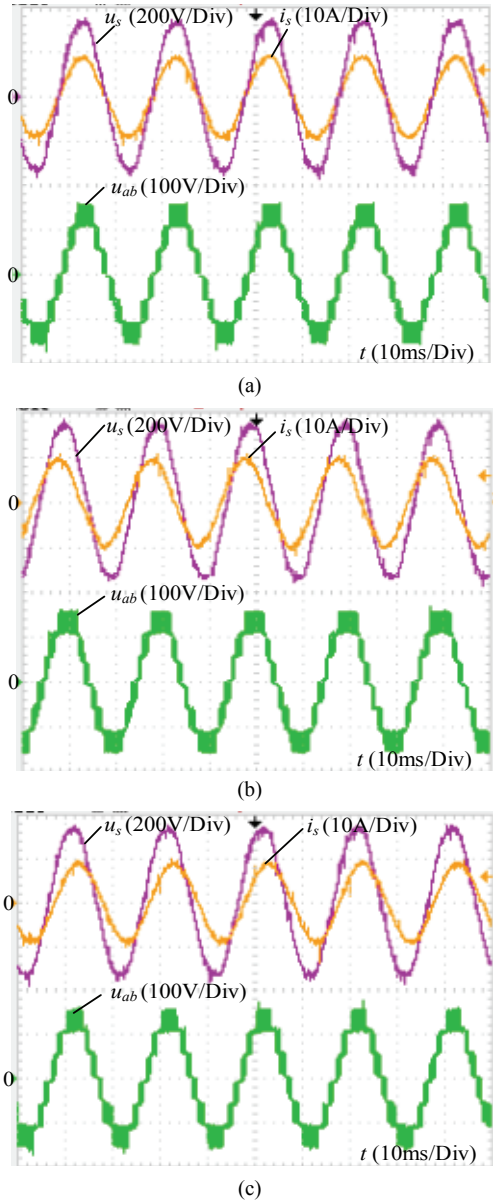

Fig. 14. Experimental results of a CHB in the steady state. (a) Unity power factor mode. (b) Capacitive mode. (c) Inductive mode.

reactive power reference is altered in the controller, the CHB can generate or absorb reactive power to the power grid. Fig. 14(a) shows a seven-level PWM voltage, a single-phase grid voltage and an input current waveform. The input current is in phase with the grid voltage, which indicates a unity power factor. As shown in Fig. 14(b), the input current is leading the grid voltage. As a result, the three-cell CHB rectifier is generating reactive power to the input. In Fig. 14(c), the input current is lagging the grid voltage. Therefore, the three-cell CHB rectifier is absorbing reactive power from the power system.

In order to verify the unbalanced-load correction capability of the above mentioned three-cell CHB rectifier, the load resistance R_3 connected to the third DC-link H-bridge is

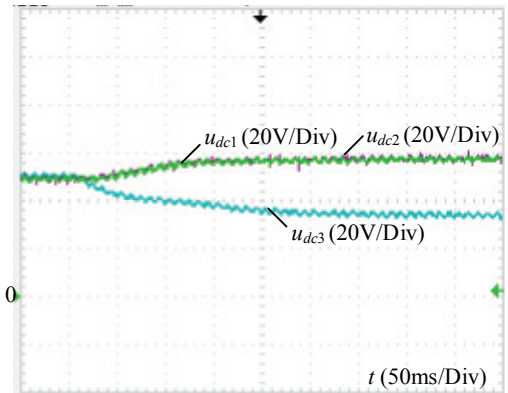

Fig. 15. DC-link voltages without balance control.

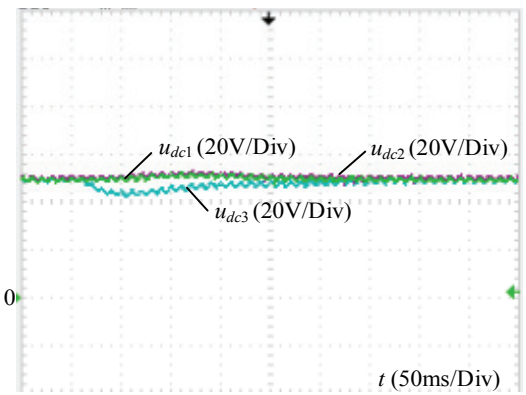

Fig. 16. DC-link voltages with balance control.

dynamically changed to form the active power differences. The load resistance R_3 changes from 15 Ω to 10 Ω, while R_1 and R_2 are kept at 15 Ω. Fig. 15 shows three DC-link voltages without the voltage balance control. The three DC-link voltages are all regulated at 50 V when the loads are the same. However, after the third load changes, the three DC-link voltages become 58 V, 58 V and 34 V. The summation of all the DC-link voltages is equal to the total reference. Fig. 16 shows three DC-link voltages with the voltage balance control. Even if the load resistance changes, the balance controller can quickly regulate the DC-link voltage u_{dc3} back to the setting. The experiment verifies the effectiveness of the voltage balance controller.

Fig. 17 examines the transient-state response with step current changes in i_{sq}^* in the αβ frame system. In Fig. 17(a), the grid voltage u_s is in phase with the input current i_s when i_{sp}^* is 9 A and i_{sq}^* is 0 A initially. The value of i_{sq}^* is stepped from 0 A to 5 A at 55 ms. In Fig. 17(b), grid voltage u_s is lagging the input current i_s when i_{sq}^* is 5 A initially. The value of i_{sq}^* is stepped from 5 A to -5 A at 45 ms. In Fig. 17(c), the grid voltage u_s is leading the input current i_s when i_{sq}^* is -5A initially. The value of i_{sq}^* is stepped from -5A to 5A at 45ms. Along with the current reference changes, the phase difference between u_s and i_s has corresponding changes. As observed in these figures, the input current i_s in the αβ frame control can exactly track the new current reference under transients. The

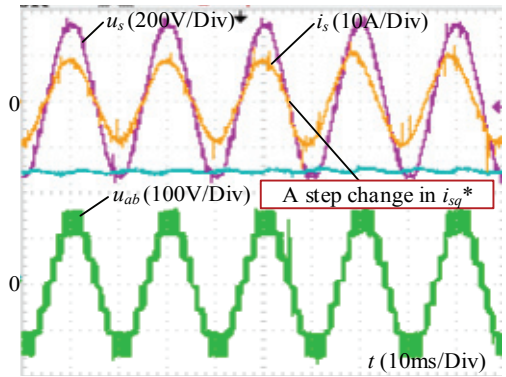

(a)

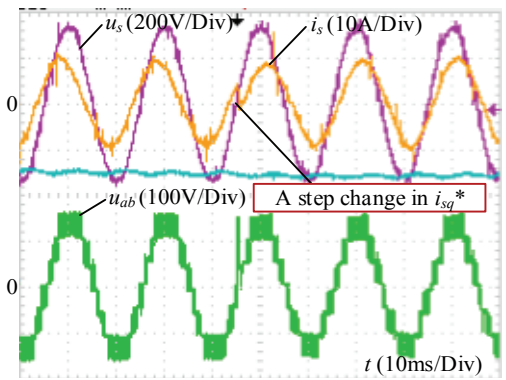

(b)

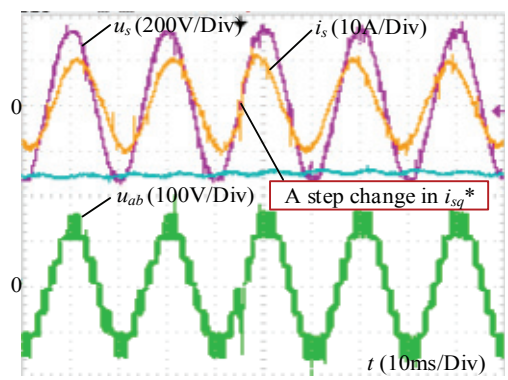

(c)

Fig. 17. Step current reference change in the inverting mode. (a) i_{sq}* from 0A to 5A. (b) i_{sq}* from 5A to -5A. (c) i_{sq}* from -5A to 5A.

obtained results confirm the correct operation of the αβ frame control during reactive current changes.

V. Conclusions

A control method in the αβ frame is introduced in this paper. The proposed method aims to resolve the DC-link voltage unbalance and power mismatch problems among H-bridges. The control method can be extended to the *N*-cell CHB rectifier stage of a SST. The following points summarize the work presented in this paper.

1) The αβ frame control structures are simple since they only need an imaginary voltage component. They do

not require an imaginary current component or a PLL.

2) Refactoring the duty cycle can achieve DC-link voltage balance and reactive power function control without a coupling effect on the original system.
3) When compared with the d-q coordinate control, the αβ frame control shows a better and faster transient-state performance.

REFERENCES

[1] A. Ipakchi and F. Albuyeh, "Grid of the future," *IEEE Power & Energy Mag*., Vol. 7, No. 2, pp. 52-62, Mar/Apr. 2009.

[2] T. Besselmann, A. Mester, and D. Dujic, "Power electronic traction transformer: Efficiency improvements under light-Load conditions," *IEEE Trans. Power Electron*., Vol. 29, No. 8, pp. 3971-3981, Aug. 2014.

[3] C. Liu, P. W. Sun, J. S. Lai, Y. C. Ji, M. Y. Wang, C. L. Chen, and G. W. Cai, "Cascade dual-boost/buck active-front-end converter for intelligent universal transformer," *IEEE Trans. Ind. Electron.*, Vol. 59, No. 12, pp. 4671-4680, Dec. 2012.

[4] E. R. Ronan, S. D. Sudhoff, S. F. Glover, and D. L. Galloway, "A power electronic-based distribution transformer," *IEEE Trans. Power Del.*, Vol. 17, No. 2, pp. 537-543, Apr. 2002.

[5] T. F. Zhao, J. Zeng, S. Bhattacharya, M. E. Baran, and A. Q. Huang, "An average model of solid state transformer for dynamic system simulation," in *Proc. IEEE Power Energy &. Gen. Meeting*, pp. 1-8, 2009.

[6] A. Q. Huang, M. L. Crow, G. T. Heydt, J. P. Zheng and S. J. Dale, "The future renewable electric energy delivery and management (FREEDM) system: The energy internet," *Proceedings of the IEEE*, Vol. 99, No. 1, pp. 133-148, Jan. 2011.

[7] X. She, X. W. Yu, F. Wang, and A. Q. Huang, "Design and demonstration of a 3.6-kV 120-V/10-kVA solid-state transformer for smart grid application," *IEEE Trans. Power Electron.*, Vol. 29, No. 8, pp. 3982-3996, Aug. 2014.

[8] T. Zhao, G. Wang, S. Bhattacharya, and A. Q. Huang, "Voltage and power balance control for a cascaded H-bridge converter-based solid-state transformer," *IEEE Trans. Power Electron*, Vol. 28, No. 4, pp. 1523-1532, Apr. 2013.

[9] J. H. Feng, W. Q. Chu, Z. X. Zhang, and Z. Q. Zhu, "Power electronic transformer-based railway traction systems: challenges and opportunities," *IEEE Trans. Power Electron.*, Vol. 5, No. 3, pp.1237-1253, Sep. 2017.

[10] B. Zhao, Q. Song, J. G. Li, Q. H. Sun, and W. H. Liu, "Full-Process operation, control, and experiments of modular high-frequency-link DC transformer based on dual active bridge for flexible MVDC distribution: a practical tutorial," *IEEE Trans. Power Electron.*, Vol. 32, No. 9, pp. 6751-6766, Sep. 2017.

[11] X. She, A. Q. Huang, and R. Burgos, "Review of solid-state transformer technologies and their application in power distribution systems," *IEEE J. Emerg. Sel. topics Power Electron.*, Vol. 1, No. 3, pp. 186-198, Sep. 2013.

[12] H. Akagi, "Classification, terminology, and application of the modular multilevel cascade converter (MMCC)," *IEEE Trans. Power Electron.*, Vol. 26, pp. 3119-3130, Nov. 2011.

[13] Y. F. Yu, G. Konstantinou, B. Hredzak, and V. G. Agelidis, "Power balance of cascaded H-Bridge multilevel converters for large-scale photovoltaic integration," *IEEE Trans. Power Electron.*, Vol. 31, No. 1, pp. 292-303, Jan. 2016.

[14] X. She, A.Q. Huang, and X. J. Ni, "Current sensorless power balance strategy for DC/DC converters in a cascaded multilevel converter based solid state transformer," *IEEE Trans. Power Electron.*, Vol. 29, No. 1, pp. 17-22, Jan. 2014.

[15] X. She, A. Q. Huang, F. Wang, and R. Burgos, "Wind energy system with integrated active power transfer, reactive power compensation, and voltage conversion functions," *IEEE Trans. Ind. Electron.*, Vol. 60, No. 10, pp. 4512-4524, Oct. 2013.

[16] Y. Liu, A. Q. Huang, W. C. Song, S. Bhattacharya, and G. J. Tan, "Small-signal model-based control strategy for balancing individual DC capacitor voltages in cascaded multilevel inverter-based STATCOM," *IEEE Trans. Ind. Electron.*, Vol. 56, No. 6, pp. 2259-2269, Jun. 2009.

[17] M. Mazuela, I. Baraia, A. Sanchez-Ruiz, I. Echeverria, I. Torre, and I. Atutxa, "Simple voltage balancing method to protect series-connected devices experimentally verified in a 5L-MPC converter," *IEEE Trans. Ind. Electron*, Vol. 65, No. 5, pp. 3699-3707, May. 2018.

[18] S. A. Khajehoddin, A. Bakhshai, and P. K. Jain, "A simple voltage balancing scheme for m-level diode-clamped multilevel converters based on a generalized current flow model," *IEEE Trans. Power Electron*., Vol. 23, No. 5, pp. 2248-2259, Sep. 2008.

[19] S. B. Monge, S. Alepuz, J. Rocabert, and J. Bordonau, "Pulsewidth modulations for the comprehensive capacitor voltage balance of n-level two-leg diode-clamped converters," *IEEE Trans. Power Electron*., Vol. 24, No. 8, pp. 1951-1959, Aug. 2009.

[20] B. P. McGrath, D. G. Holmes, and W. Y. Kong, "A decentralized controller architecture for a cascaded H-bridge multilevel converter," *IEEE Trans. Ind. Electron*., Vol. 61, No. 3, pp. 1169-1178, Mar. 2014.

[21] C. Han, A. Q. Huang, Yu. L, and B. Chen, "A generalized control strategy of per-phase DC voltage balancing for cascaded multilevel converter-based STATCOM," *in Proc. IEEE Power Electron. Spec. Conf*, pp. 1746-1752, 2007.

[22] X. Y. Wang, J. J. Liu, S. D. Ouyang, and F. Meng, "Research on unbalanced-load correction capability of two power electronic transformer topologies," *IEEE Trans. Power Electron.*, Vol. 30, No. 6, pp.3044-3056, Jun. 2015.

[23] X. She, A .Q. Huang, T. F. Zhao, and G. Y. Wang, "Coupling effect reduction of a voltage-balancing controller in single-phase cascaded multilevel converters," *IEEE Trans. Power Electron.*, Vol. 27, No. 8, pp. 3530-3543, Aug. 2012.

[24] G. Farivar, B. Hredzak, and V. G. Agelidis, "Decoupled control system for cascaded H-Bridge multilevel converter based STATCOM," *IEEE Trans. Ind. Electron.*, Vol. 63, No. 1, pp.322-331, Jan. 2016.

[25] D. S. Sha, G. Xu, and Y. X. Xu, "Utility direct interfaced charger/discharger employing unified voltage balance control for cascaded H-Bridge units and decentralized control for CF-DAB modules," *IEEE Trans. Ind. Electron.*, Vol. 64, No. 10, pp. 7831-7841, Oct. 2017.

[26] J. A. Barrena, L. Marroyo, M. A. R. Vidal, and J. R. T. Apraiz, "Individual voltage balancing strategy for PWM

cascaded H-bridge converter based STATCOM," *IEEE Trans. Ind. Electron.*, Vol. 55, No. 1, pp. 21-29, Jan. 2008.
[27] D. L. Yang, N. Wu, L. Yin, and Z. G. Lu, "Natural frame control of single-phase cascaded H-Bridge multilevel converter based on fictive-phases construction," *IEEE Trans. Ind. Electron.*, Vol. 65, No. 5, pp. 3848-3857, May. 2018.
[28] S. Somkun and V. Chunkag, "Unified unbalanced synchronous reference frame current control for single-phase grid-connected voltage source converters," *IEEE Trans. Ind. Electron*., Vol. 63, No. 9, pp. 5425-5436, Sep. 2016.

Hui Wong was born in China, in 1992. She received her B.S. degree in Electronics Engineering from Anhui University of Science and Technology, Huainan, China, in 2016. She is presently working towards her M.S. degree in Electrical Engineering at Guangxi University, Nanning, China. Her current research interests include digital signal processing based control applications, PWM converter/inverter systems and DC-DC converters.

Wendong Huang was born in China, in 1992. He received his B.S. degree from the Department of Electrical Engineering of Southwest Jiaotong University (Emei Campus), Sichuan, China, in 2016. He is presently working towards his M.S. degree in Electrical Engineering in the College of Electrical Engineering, Guangxi University, Nanning, China. His current research interests include power quality compensation systems such as STATCOM, APF and SVG devices.

Li Yin was born in China, in 1994. He received his B.S. degree in Electrical Engineering and Automation from Guangzhou University, Guangzhou, China, in 2016. He is presently working towards his M.S. degree in the College of Electrical Engineering, Guangxi University, Nanning, China. His current research interests include power quality and solid-state transformers.